How to cite: *Angew. Chem. Int. Ed.* **2023**, *62*, e202309790
doi.org/10.1002/anie.202309790

Reactivity Hot Paper

Pushing the Upper Limit of Nucleophilicity Scales by Mesoionic *N*-Heterocyclic Olefins

Andreas Eitzinger[+], *Justus Reitz*[+], *Patrick W. Antoni, Herbert Mayr, Armin R. Ofial,* and Max M. Hansmann**

Abstract: A series of mesoionic, 1,2,3-triazole-derived *N*-heterocyclic olefins (mNHOs), which have an extraordinarily electron-rich exocyclic CC-double bond, was synthesized and spectroscopically characterized, in selected cases by X-ray crystallography. The kinetics of their reactions with arylidene malonates, $ArCH{=}C(CO_2Et)_2$, which gave zwitterionic adducts, were investigated photometrically in THF at 20 °C. The resulting second-order rate constants k_2(20 °C) correlate linearly with the reported electrophilicity parameters E of the arylidene malonates (reference electrophiles), thus providing the nucleophile-specific N and s_N parameters of the mNHOs according to the correlation lg k_2(20 °C)$=s_N(N+E)$. With $21<N<32$, the mNHOs are much stronger nucleophiles than conventional NHOs. Some mNHOs even excel the reactivity of mono- and diacceptor-substituted carbanions. It is exemplarily shown that the reactivity parameters thus obtained allow to calculate the rate constants for mNHO reactions with further Michael acceptors and predict the scope of reactions with other electrophilic reaction partners including carbon dioxide, which gives zwitterionic mNHO-carboxylates. The nucleophilicity parameters N correlate linearly with a linear combination of the quantum-chemically calculated methyl cation affinities and buried volumes of mNHOs, which offers a valuable tool to tailor the reactivities of strong carbon nucleophiles.

Introduction

Electron-donating or -withdrawing substituents strongly influence the reactivity of olefinic π-systems. One concept to generate strong neutral carbon nucleophiles relies on the ylidic polarization of π-systems by geminal substitution with donor groups. In ketene-*N*,*N*-acetals (1,1-enediamines) **A1**,[1] for example, two dialkylamino groups transfer electron density towards the olefinic π-bond (Scheme 1). The electron-donating effect of the two amino groups can be further enhanced by embedding them in conformationally rigid heterocycles (**A2**) (Scheme 1).[2,3] Such strongly polarized *N*-heterocyclic olefins (NHOs) can be represented by a neutral (**A2**) or a zwitterionic Lewis structure (**A2′**), in which the exocyclic methylene unit bears a negative charge. NHOs have found plenty of applications due to their strong donor properties[4] ranging from organocatalysis,[5] over main group chemistry[6] to polymer chemistry.[7] Their basicity as well as nucleophilicity are remarkably high and exceed in many cases those of *N*-heterocyclic carbenes (NHCs).[8]

In 2020, the Hansmann group introduced a new concept to generate strong carbon donors based on mesoionic carbon-carbon bond polarization.[9] Such mesoionic methylides or mesoionic *N*-heterocyclic olefins (mNHOs) based on 4-methylene 1,3-imidazoles or 4-methylene 1,2,3-triazoles (**A3**) cannot be described through neutral but only through a series of zwitterionic Lewis structures (Scheme 1).[10,11] Competition experiments as well as the Tolman electronic parameters (TEPs) showed that the donor properties of exocyclic methylene groups of mNHOs outperform those of analogous $=CH_2$ groups of classical NHOs.[9]

[*] Dr. A. Eitzinger,[+] Prof. Dr. H. Mayr, Dr. A. R. Ofial
Department Chemie, Ludwig-Maximilians-Universität München, Butenandtstr. 5–13 (Haus F), 81377 München (Germany)
E-mail: ofial@lmu.de
J. Reitz,[+] P. W. Antoni, Jun.-Prof. M. M. Hansmann
Fakultät für Chemie und Chemische Biologie, Technische Universität Dortmund
Otto-Hahn-Str. 6, 44227 Dortmund (Germany)
E-mail: max.hansmann@tu-dortmund.de
[+] These authors contributed equally to this work.

© 2023 The Authors. Angewandte Chemie International Edition published by Wiley-VCH GmbH. This is an open access article under the terms of the Creative Commons Attribution License, which permits use, distribution and reproduction in any medium, provided the original work is properly cited.

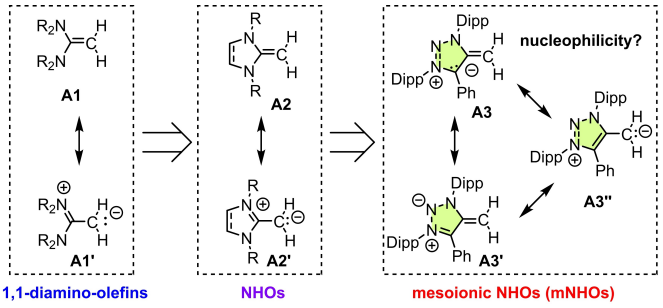

Scheme 1. Structural evolution of strong carbon-centered donors: From acyclic 1,1-diamino-olefins over NHOs to mNHOs (Dipp = 2,6-diisopropylphenyl).

© 2023 The Authors. Angewandte Chemie International Edition published by Wiley-VCH GmbH

Rapidly after their first report, the new mNHOs **A3** and analogous imidazole derivatives were applied for the synthesis of room-temperature stable diazoalkenes by the reaction with N_2O,[12] in organocatalysis,[13] and in coordination chemistry.[14] Furthermore, the triazole-derived mNHOs were reported to undergo (4+1) cycloaddition reactions with diazoesters,[15] and quantum chemical (DFT) calculations predicted the use of mNHOs for the decomposition of the greenhouse gas SF_6.[16]

In previous work by Cheng and co-workers[8f] the reactivity of conventional NHOs in THF was quantified by kinetic measurements and the application of equation (1).

$$\lg k_2(20\,^{\circ}\mathrm{C}) = s_N(N+E) \qquad (1)$$

In the linear free energy relationship (1), electrophiles are characterized by an electrophilicity parameter E, and the reactivities of nucleophiles are described by two solvent-dependent parameters, the nucleophilicity N and the sensitivity s_N.[17,18] With eq. (1), second-order rate constants of reactions of nucleophiles with electrophiles can usually be predicted with an accuracy of two orders of magnitude in a reactivity range of 40 orders of magnitude.[17d] In order to explore the synthetic potential of mNHOs, i.e., to efficiently identify potential electrophilic reaction partners and to create a basis to design novel mNHOs with specific reactivities, we now determined their N and s_N parameters by studying the kinetics of their reactions with well-established reference electrophiles.

Results and Discussion

Synthesis and Characterization of mNHOs

The synthesis of a series of novel mNHOs was achieved by deprotonation of 4-methyl-1,2,3-triazolium hexafluorophosphates or iodides, which are accessible by two synthetic pathways (Scheme 2). For 1,3-diaryl substituted derivatives we utilized the direct oxidative (3+2) cycloaddition of triazenes with alkynes (route A),[19] reported previously for **1c** and **1f**.[9] For 1,3-dialkyl-substituted triazolium salts a stepwise synthesis via methylation of the previously unknown 1,3-diisopropyl-substituted 1,2,3-triazol-5-ylidenes[20] was chosen (route B).[21] Deprotonation of the triazolium salts with potassium bis(trimethylsilyl)amide (KHMDS) cleanly afforded the corresponding mNHOs **1a–1h** in high yields. Electron accepting (**1a**, **1b**) as well as electron donating (**1d**) and sterically encumbered (**1e**) substituents R′ were tolerated.

The sterically bulky *N*-Dipp groups are not necessarily required to obtain stable mNHOs, and their synthesis can also be accomplished with *N*-^{i}Pr groups (**1g**). Even fully alkyl substituted mNHOs are synthetically accessible, as exemplified by the isolation of mNHO **1h**. The ^{13}C NMR chemical shifts for the exocyclic $=CH_2$ moiety in **1a–1h** are in a range of 48.3–39.6 ppm, significantly high field shifted compared to regular terminal olefins. Crystallization of mNHO **1g** furnished single crystals suitable for X-ray diffraction.[21,22] The crystal structure analysis shows that the C1–C2 bond length [1.368(2) Å] of **1g** is much longer than that of structurally comparable olefins (Scheme 2 and Figure S32).[21]

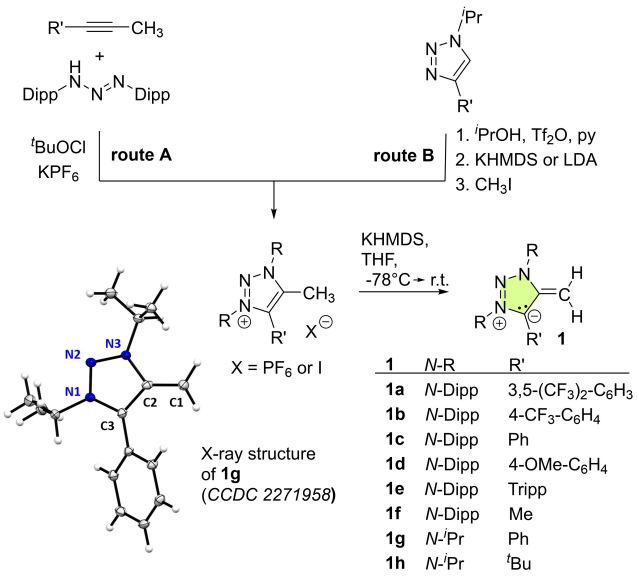

Scheme 2. Synthetic routes to triazole-derived mNHOs **1a–1h** (Dipp = 2,6-diisopropylphenyl, Tripp = 2,4,6-triisopropylphenyl). Bottom left: X-ray solid-state structure of mNHO **1g**. Thermal ellipsoids (at 100 K) are shown at the 50% probability level. Selected bond lengths (in Å): C1–C2 1.368(2); C2–C3 1.431(2); C3–N1 1.355(2); N1–N2 1.317(2); N2–N3 1.356(2).

Whereas conventional NHOs are typically colorless solids,[4] the mesoionic NHOs **1** were isolated as intensely colored compounds under inert atmosphere. The absorption maximum of mNHOs varies and shifts bathochromically with decreasing electron density (Figure 1A, B). As shown in Figure 1C, the absorption maxima of mNHOs, λ_{max},

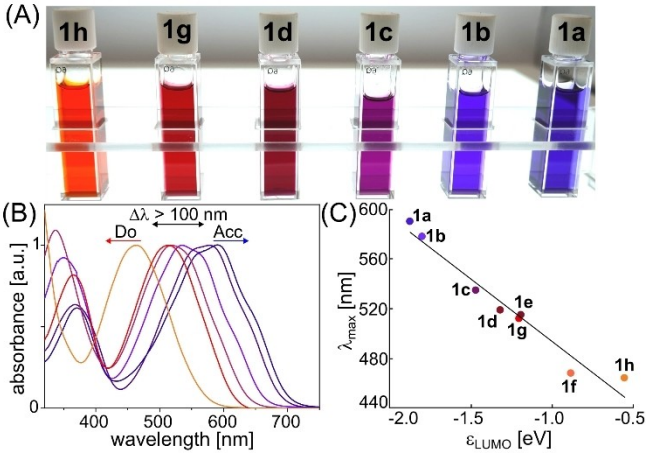

Figure 1. (A) Optical appearance of solutions of mNHOs **1a–1h** in THF as well as (B) their UV/Vis spectra in THF and (C) the linear correlation of λ_{max} with ε_{LUMO}.

© 2023 The Authors. Angewandte Chemie International Edition published by Wiley-VCH GmbH

15213773, 2023, 40, Downloaded from https://onlinelibrary.wiley.com/doi/10.1002/anie.202309790 by Technische Universiteit Dortmund Dezernat Finanzen und Beschaffung, Wiley Online Library on [18/11/2024]. See the Terms and Conditions (https://onlinelibrary.wiley.com/terms-and-conditions) on Wiley Online Library for rules of use; OA articles are governed by the applicable Creative Commons License

correlate linearly with the energy of the LUMO, ε_{LUMO} (Figure 1C).[21]

The mNHOs are highly air-sensitive compounds as indicated by rapid decolorization at air. However, when stored under an inert atmosphere, the mNHOs **1a**–**1f** persist for days, both in solution as well as in the solid state. The *N*-alkyl substituted mNHOs **1g** and **1h** are more prone to decomposition (e.g., they degrade when heated at 50 °C), but are stable at room temperature for at least 24 h under inert atmosphere.[21]

Kinetic Experiments—Nucleophilicities of mNHOs

When selecting reference electrophiles for the determination of mNHO nucleophilic reactivities, we used Michael acceptors whose electrophilicities *E* had previously been reliably characterized.[18] Hence, the product studies depicted in Scheme 3 mainly served to identify Michael acceptors that would enable us to determine the nucleophilicity parameters *N* and s_N of the mNHOs **1** from the kinetics of carbon-carbon bond-forming reactions between mNHOs and electrophiles.

First, we investigated the reactions of *N*-aryl and *N*-alkyl substituted mNHOs **1c** and **1g** with *p*-quinone methides (*p*QMs) **4a** and **4b** in THF. The products were isolated in 52–88 % yield as zwitterions **6a**–**6c** and analyzed spectroscopically. The *p*QM/mNHO adduct **6a** was additionally characterized by X-ray diffraction.[21,22] However, several combinations showed significant superimposition of the UV/Vis absorptions of NHOs and *p*QMs, which prevented the photometric determination of their reaction kinetics.

The arylidene malonates **5a**–**5h** constitute another series of weakly reactive Michael acceptors ($E = -17.7$ to -23.8) that were previously suggested as reference electrophiles for the characterization of highly reactive nucleophiles.[23] As depicted in Scheme 3, the reactions of arylidene malonates **5** with mNHOs **1c** or **1g** furnished the zwitterionic adducts **7a**–**7c**, which were fully characterized by spectroscopic methods and in case of **7c** additionally by X-ray crystallography.[21,22] Even the reaction of the sterically hindered ^{t}Bu-substituted mNHO **1h** with the weak electrophile **5h** ($E = -23.80$) afforded the corresponding addition product **7d**. Since their UV/Vis absorptions overlap only little with those of mNHOs **1** we used the Michael acceptors **5** as reference electrophiles to characterize the nucleophilicities of the electron-rich mNHOs **1** through kinetic studies.

Assuming analogous reaction paths for all other mNHO/arylidene malonate combinations, the kinetics of the adduct formation between the mNHOs **1** and the reference electrophiles **5** in THF (20 °C) were monitored spectrophotometrically by following the decay of the UV/Vis absorbances of one of the two colored reaction partners at their λ_{max} using stopped-flow techniques. Under pseudo-first order conditions (one of the reaction partners was used in at least 4-fold excess), the first-order rate constants k_{obs} (s^{-1}) were obtained by least-squares fitting of the exponential function $A_t = A_0 \exp(-k_{obs}t) + C$ to the experimentally observed decay of the time-dependent absorbances. For each combination of mNHO **1** with **5**, k_{obs} was determined at four different concentrations of the compound used in excess, which allowed us to calculate the second-order rate constants k_2 ($M^{-1}s^{-1}$) from the slopes of the linear correlations of k_{obs} with the concentration of the excess component. The workflow of this procedure is visualized in Figure 2 for the combination of **5c** and **1b**. Details of all kinetic measurements are gathered in the Supporting Information. A compilation of determined second-order rate constants k_2 is provided in Table 1.

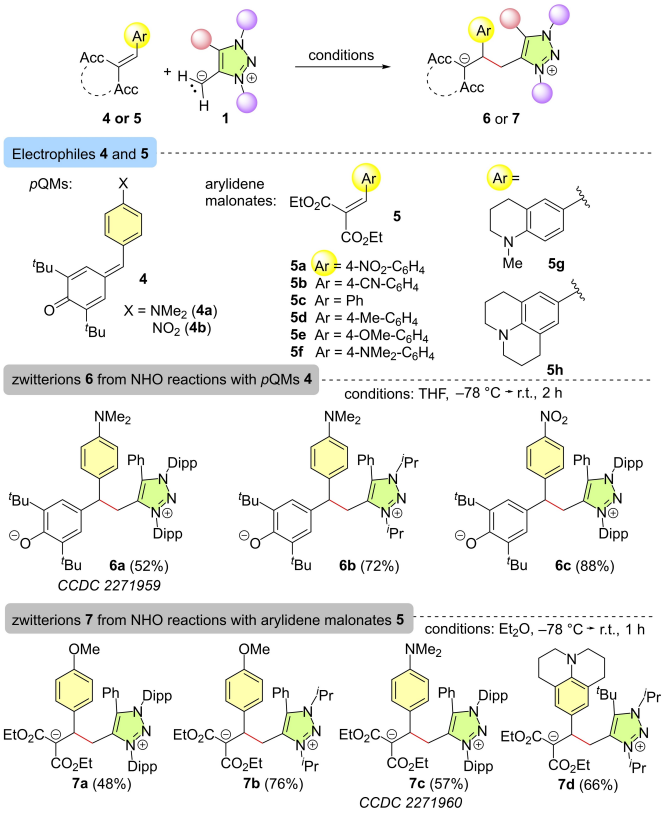

Scheme 3. Reactivity of mNHOs **1** towards electron-deficient olefins **4** or **5** (yields refer to isolated, crystallized products).

Correlation Analysis

In Figure 3, the decadic logarithm of second-order rate constants (lg k_2) of reactions of mNHOs **1a**–**1h** with the electrophiles **5** (and **8**) are plotted against the previously reported electrophilicity parameters *E*. From the linear correlations the nucleophilicities *N* and nucleophile-specific sensitivity parameters s_N of the mNHOs **1** in THF were calculated using eq. (1) and listed in Table 1.

The nucleophile-specific susceptibilities s_N fall within a narrow range (0.42 to 0.61), implying that the relative reactivities of mNHOs **1** towards electrophiles **5** depend only slightly on the electrophilicity of the reaction partner.

Installing *N*-alkyl instead of *N*-aryl substituents at the triazole ring increases drastically the reactivity of mNHOs. As illustrated in Figure 3, mNHO **1g** (*N*-R = *N*-^{i}Pr) reacts

© 2023 The Authors. Angewandte Chemie International Edition published by Wiley-VCH GmbH

15213773, 2023, 40, Downloaded from https://onlinelibrary.wiley.com/doi/10.1002/anie.202309790 by Technische Universitaet Dortmund Dezernat Finanzen und Beschaffung, Wiley Online Library on [18/11/2024]. See the Terms and Conditions (https://onlinelibrary.wiley.com/terms-and-conditions) on Wiley Online Library for rules of use; OA articles are governed by the applicable Creative Commons License

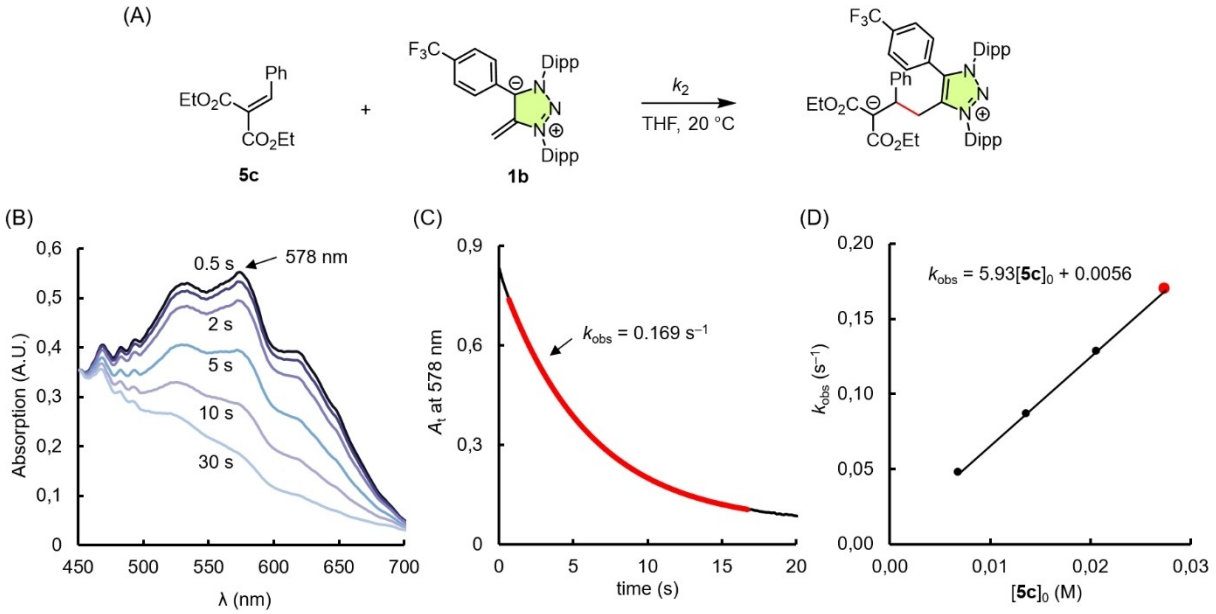

Figure 2. (A) Workflow of kinetic measurements exemplified for the reaction of **1b** with **5c** in THF at 20 °C. (B) Changes in the UV/Vis-absorption spectrum during the reaction of mNHO **1b** and arylidene malonate **5c** in THF. (C) Monoexponential decay of the absorbance of **1b** at λ_{max} = 578 nm in the reaction with **5c** ($[\mathbf{5c}]_0$ = 27.5 mM). (D) Determination of the second-order rate constant k_2 = 5.93 $M^{-1}\,s^{-1}$ from the slope of the linear correlation of first-order rate constants k_{obs} (s^{-1}) with $[\mathbf{5c}]_0$.

Table 1: Second-order rate constants k_2 ($M^{-1}\,s^{-1}$) for the reactions of mNHOs **1a–1h** with the diethyl arylidene malonates **5a–5h** (and ethyl cinnamate **8**) in THF at 20 °C as well as nucleophile-specific reactivity parameters *N* and s_N of mNHOs **1a–1h**.

Electrophiles	Electrophilicity E[a]	k_2 ($M^{-1}\,s^{-1}$)							
		1a	**1b**	**1c**	**1d**	**1e**	**1f**	**1g**	**1h**
5a	−17.67	–	2.07×10^{2}	1.15×10^{3}	2.46×10^{3}	8.11×10^{1}	5.16×10^{3}	–	–
5b	−18.06	2.48×10^{1}	1.19×10^{2}	6.73×10^{2}	1.14×10^{3}	4.19×10^{1}	3.30×10^{3}	–	–
5c	−20.55	–	5.93	2.36×10^{1}	–	–	–	–	–
5d	−21.11	1.36	–	1.07×10^{1}	2.03×10^{1}	6.36×10^{-1}	1.11×10^{2}	1.06×10^{5}	–
5e	−21.47	8.04×10^{-1}	2.25	5.68	–	3.79×10^{-1}	4.60×10^{1}	5.21×10^{4}	–
5f	−23.10	1.90×10^{-1}	4.90×10^{-1}	–	2.02	–	–	9.39×10^{3}	–
5g	−23.40	–	–	–	–	–	–	4.50×10^{3}	2.48×10^{4}
5h	−23.80	–	–	–	–	–	-	3.38×10^{3}	1.97×10^{4}
8[b]	−24.52	–	–	–	–	–	–	–	6.77×10^{3}
N (s_N)		21.36 (0.42)	22.30 (0.49)	22.80 (0.60)	23.55 (0.56)	20.78 (0.61)	24.86 (0.52)	30.25 (0.54)	31.92 (0.52)

[a] Taken from refs. [18, 23]. [b] For the highly reactive mNHO **1h**, k_2 of the reaction with ethyl cinnamate (**8**) was also considered for the determination of *N* and s_N.

10,000 times faster than the otherwise identical *N*-Dipp derivative **1c**.

An interplay of steric and electronic factors accounts for these results. As indicated by X-ray structural analysis and quantum-chemical calculations,[21] the sterically demanding *N*-Dipp substituents are orthogonally oriented to the triazole plane. For that reason, these aryl rings act as electron acceptors and account for the fact that mNHOs with *N*-Dipp (**1a–1f**) are less nucleophilic than those with *N*-^{i}Pr substituents (**1g**, **1h**). Steric shielding by the Tripp-substituent in 5-position (**1e**) leads to an even lower nucleophilicity (N = 20.78).

Figure 4A illustrates that second-order rate constants (lg k_2) for mNHO reactions with **5** correlate linearly with Hammett substituent constants σ[24] of aromatic substituents at **5**. Given that also the nucleophilicities *N* of 5-aryl-sustituted mNHOs **1a–1d** correlate well with Hammett's σ (Figure 4B), a straightforward prediction of the reactivities of so far unknown mNHOs with analogous structures becomes feasible. A classical Hammett plot of lg k_2(**5b**) vs. σ for mNHOs **1a–1d** gives a linear relationship (r^2 = 0.98) with a slope of −1.46, which corresponds to the Hammett reaction constant ρ.

The comparison of the reactivities of mNHOs **1a–1h** with other nucleophilic compounds in Figure 5 shows that the *N*-alkyl substituted mNHOs are even more reactive than pyridinium ylides and weakly stabilized carbanions, so far the most reactive compounds in the nucleophilicity scale.[18]

© 2023 The Authors. Angewandte Chemie International Edition published by Wiley-VCH GmbH

15213773, 2023, 40, Downloaded from https://onlinelibrary.wiley.com/doi/10.1002/anie.202309790 by Technische Universiteit Dortmund Dezernat Finanzen und Beschaffung, Wiley Online Library on [18/11/2024]. See the Terms and Conditions (https://onlinelibrary.wiley.com/terms-and-conditions) on Wiley Online Library for rules of use; OA articles are governed by the applicable Creative Commons License

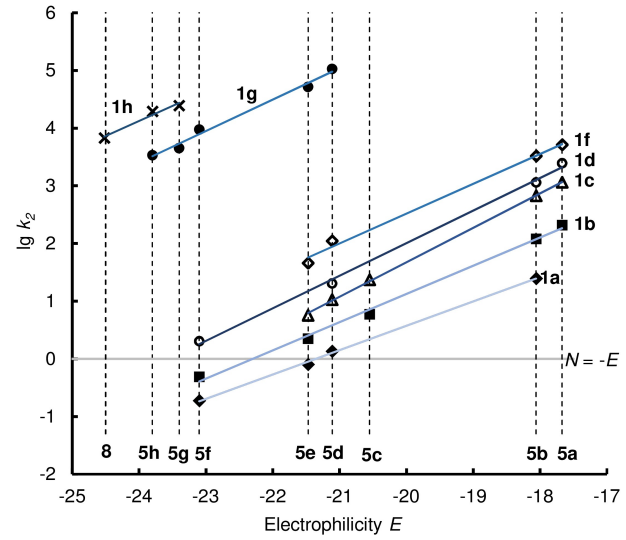

Figure 3. Linear relationships of lg k_2 of reactions of mNHOs **1a–1h** with the reference electrophiles **5** (and **8**) in THF at 20 °C with the electrophilicity parameters E of **5** (and **8**); the correlation for **1e** is shown in the Supporting Information.

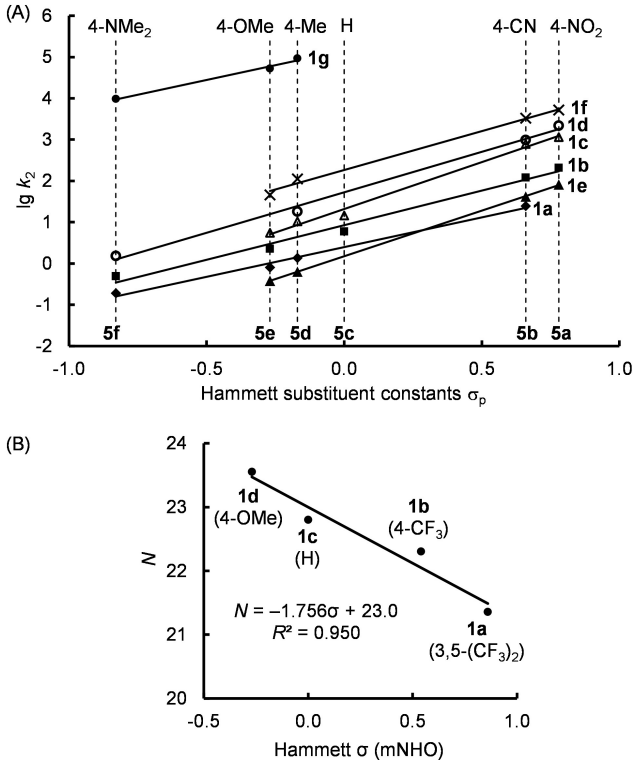

Figure 4. (A) Linear correlations of lg k_2 for the reactions **1** + **5** in THF at 20 °C with the Hammett substituent constants σ_p of **5**. (B) Linear relationship of Mayr N (from Table 1) with Hammett σ for mNHOs **1a–1d**.

The nucleophilicities of the *N*-Dipp derivatives lie in the same range as those of the most reactive NHCs, such as IMes and SIMes, and exceed those of classical NHOs or other commonly used nucleophilic catalysts (in THF) by

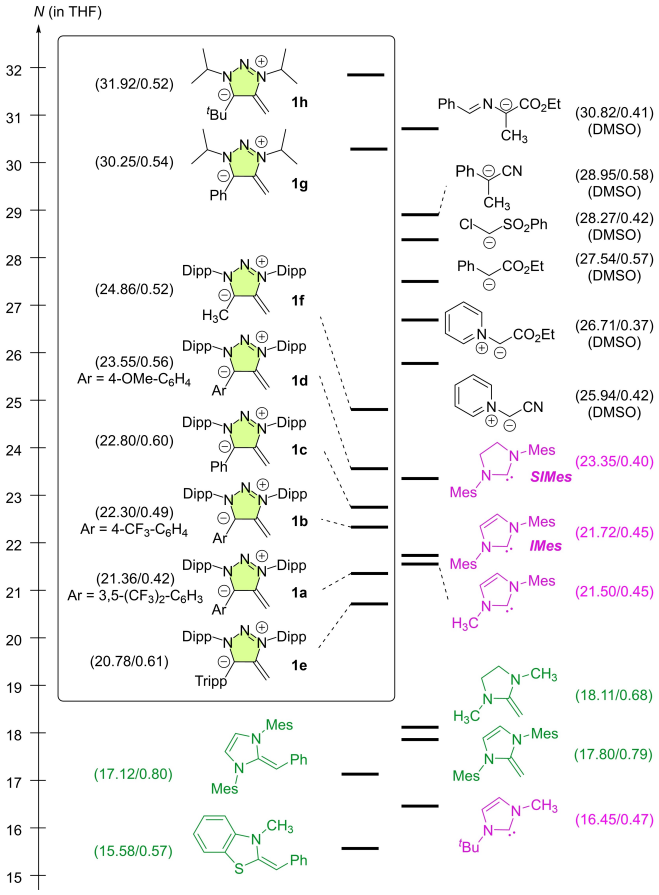

Figure 5. Embedding mNHOs **1a–1h** in the nucleophilicity scale (N/s_N values in parentheses were taken from ref. [18] and refer to reactions in THF if not indicated otherwise).

several units (for example: $N = 16.12$ for DBU; 15.90 for DMAP; 13.59 for Ph_3P).[18] The quantification of mNHO reactivities can now be used to predict reaction times with various types of electrophiles or novel mNHO/electrophile combinations for synthetic applications.

Scope of mNHO Reactions with Further Types of Electrophiles

Further Michael Acceptors. The formation of adducts from mNHOs and *p*QMs **4a** ($E = -17.29$)[18] and **4b** ($E = -14.36$)[18] depicted in Scheme 3 is in line with the prediction of fast reactions by equation (1). As illustrated in Figure 3, we could even use the second-order rate constant $k_2(20\,°C) = 6.77\times10^3\ M^{-1}s^{-1}$ of the reaction **1h** + **8** to extend the linear correlation formed by the data points for the kinetics of **1h** with the arylidene malonates **5g** and **5h**.

Based on their high nucleophilicities N, all mNHOs **1** are expected to undergo fast reactions with most electrophiles in Mayr's database of reactivity parameters, which currently covers reactivities down to $E = -29.6$ (for 3-methylcyclohex-2-en-1-one).[18] For example, a rate constant of 0.1 $M^{-1}\,s^{-1}$ is predicted by equation (1) for the reaction of mNHO **1c** with the weak electrophile **8** ($E = -24.52$). The reaction of **1c**

© 2023 The Authors. Angewandte Chemie International Edition published by Wiley-VCH GmbH

15213773, 2023, 40, Downloaded from https://onlinelibrary.wiley.com/doi/10.1002/anie.202309790 by Technische Universiteit Dortmund Dezernat Finanzen und Beschaffung, Wiley Online Library on [18/11/2024]. See the Terms and Conditions (https://onlinelibrary.wiley.com/terms-and-conditions) on Wiley Online Library for rules of use; OA articles are governed by the applicable Creative Commons License

with ethyl cinnamate **8** in THF accordingly furnished the addition product which tautomerizes into **9** (Scheme 4A).[21] Isolated single crystals of (*E*)-**9** were suitable for X-ray diffraction, which confirmed its mesoionic structure. Consequently, the exocyclic π-bond in **9** has a reduced double bond character, which explains the observation of an (*E*/*Z*)-mixture in the NMR spectra when crystalline (*E*)-**9** is dissolved in d_6-benzene.[21,22]

Electrophile **10** (approx. $E=-9$ to -10) is known to react with secondary amines to Stenhouse adducts by amine attack at the furyl ring and subsequent ring-opening.[25] In contrast, the mNHO addition of **1c** to the electron-deficient CC double bond of **10** gave **11** (Scheme 4B). Also, arylidene malononitrile **12** ($E=-13.30$)[18] underwent a smooth classical Michael addition with mNHO **1c** to furnish **13** in high yield (Scheme 4C).

Table 2 shows that the experimental rate constants (k_2^{exp}) for the reactions of the weakly reactive mNHO **1a** with *tert*-butyl acrylate (**14**) and the *β*-nitrostyrene **15** as well as for the adduct formation of the highly reactive mNHO **1h** with cinnamonitrile (**16**) agree with those calculated by equation (1) within a factor of 6. It can, therefore, be expected that the mNHO nucleophilicity parameters reported in Table 1 allow one to generally predict the rates of mNHO reactions with ordinary Michael acceptors with a precision of approximately one order of magnitude.

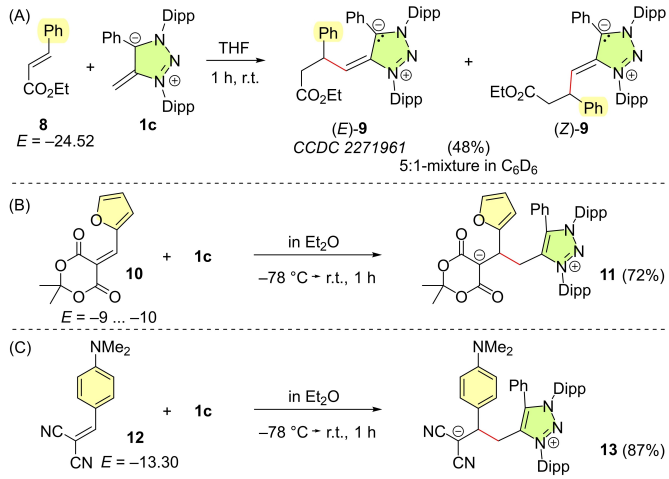

Scheme 4. Reactivity of mNHOs **1** towards Michael acceptors (A) **8**, (B) **10** and (C) **12** (yields refer to isolated products).

Table 2: Kinetics of reactions of mNHOs with further Michael acceptors (in THF at 20 °C).

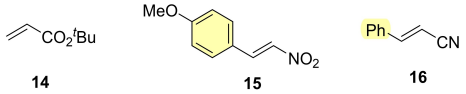

mNHOs	Electrophiles (*E*)	k_2^{exp} (M^{-1} s^{-1})	k_2^{eq1} (M^{-1} s^{-1})	k_2^{exp}/k_2^{eq1}
1a	**14** (−20.22)[a]	1.77	3.0[b]	1/1.7
1a	**15** (−14.70)[a]	3.81×10^3	6.3×10^2 [b]	6.1
1h	**16** (−24.60)[a]	8.82×10^3	6.4×10^3 [b]	1.4

[a] Electrophilicity parameters *E* from ref. [18]. [b] Second-order rate constants k_2^{eq1} calculated by substituting the reactivity parameters *E*, *N* and s_N in eq. 1.

Electrophilic Fluorination. We further challenged the use of equation (1) for mNHOs by combining the reactivity parameters for mNHO **1c** ($N=22.80$, $s_N=0.60$) with the reactivity parameter $E=-8.44$ of the electrophilic fluorination reagent NFSI (**17**).[26] With these reactivity data at hand, we predicted a rapid formation ($k_2\approx10^8\,M^{-1}s^{-1}$) of the fluoromethyl-substituted triazolium salt **18** at room temperature. In accord with our expectations and without further optimization, mixing **1c** and **17** in toluene at room temperature furnished salt **18** in a yield of 68 % within 15 min (Scheme 5).

CO_2 Fixation. Many conventional NHOs have been described to form adducts with carbon dioxide,[4d,27] for which an $E=-16.3$ was estimated from its reactivity toward the indenide anion.[28] Since the mNHOs are stronger nucleophiles than ordinary NHOs, we expected that mNHOs also form adducts with CO_2. This anticipation was realized by the observation that the *N*-aryl and *N*-alkyl substituted mNHOs **1c** and **1g**, respectively, furnished the zwitterionic triazolium carboxylates **19a** and **19b** in good yields (Scheme 6). The newly formed CC bond in **19a** (*N*-Dipp) appeared to be weak and heating at 50 °C as well as applying vacuum triggered the loss of CO_2 and regeneration of the mNHO **1c**.[21] As a consequence, **19a** was dried under a stream of CO_2. Under an atmosphere of CO_2, crystals suitable for single-crystal X-ray analysis could be obtained.[21,22] The length of the C–CO_2 bond in **19a** [1.5708 (18) Å] is similar to that in CO_2 adducts of NHOs [1.549(3)–1.598(6) Å].[27]

In contrast, **19b**, the CO_2 adduct of **1g** (*N*-^{i}Pr), is stable at elevated temperatures or under vacuum. Thus, the CO_2 binding studies suggest that **1g** (with *N*-^{i}Pr) is a considerably stronger Lewis base than **1c** (with *N*-Dipp) paralleling with the nucleophilicity order for these two mNHOs, which is **1g** > **1c**.

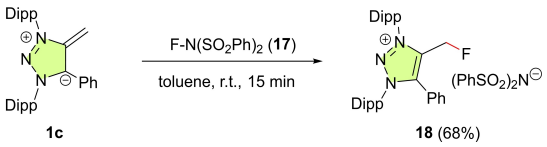

Scheme 5. Fluorination of **1c** by NFSI (**17**).

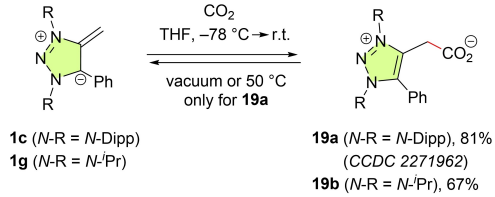

Scheme 6. Reactivity of mNHOs **1c** and **1g** towards CO_2. The reversibly formed mNHO carboxylate **19a** was characterized by single crystal X-ray structure determination (refs. [21,22]).

© 2023 The Authors. Angewandte Chemie International Edition published by Wiley-VCH GmbH

15213773, 2023, 40, Downloaded from https://onlinelibrary.wiley.com/doi/10.1002/anie.202309790 by Technische Universitaet Dortmund Dezernat Finanzen und Beschaffung, Wiley Online Library on [18/11/2024]. See the Terms and Conditions (https://onlinelibrary.wiley.com/terms-and-conditions) on Wiley Online Library for rules of use; OA articles are governed by the applicable Creative Commons License

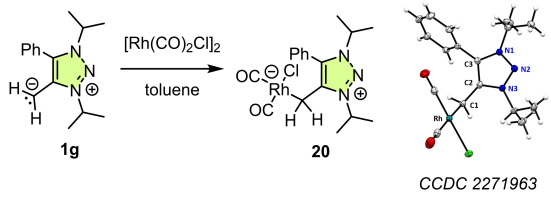

Scheme 7. Preparation of the rhodium-carbonyl complex **20** including its X-ray solid-state structure. Thermal ellipsoids are shown with 50% probability (refs. [21,22]).

Tolman Electronic Parameters of mNHOs

The overall donor properties of mNHO ligands **1c** and **1f** have previously been characterized by the Tolman electronic parameter (TEP), which is derived for a given ligand L from the IR carbonyl stretching frequencies in $[(L)RhCl(CO)_2]$ complexes.[29] To compare the donor properties of **1g** with those of **1c**[9] and **1f**[9] we prepared the rhodium carbonyl complex **20** from **1g** and rhodium carbonyl chloride (Scheme 7). After unambiguously characterizing the structure of **20** by X-ray diffraction we determined the IR spectral data. In dichloromethane solution the IR carbonyl stretching frequencies of **20** are at $\nu = 2053.1$ and 1970.6 cm^{-1}. The averaged value $\nu_{av} = 2011.9\ cm^{-1}$ for **20** which corresponds to $TEP = 2029.7\ cm^{-1}$ (calculated based on $TEP = 0.8001\ \nu_{av} + 420\ cm^{-1}$)[29] is significantly below those for strong carbon donors such as NHCs ($\nu_{av} \approx 2038\ cm^{-1}$)[29] and indicates that mNHO **1g** is an extraordinarily strong donor ligand. Interestingly, the ν_{av} value for **20** is nearly identical to those reported for the analogous $[(mNHO)RhCl(CO)_2]$ complexes of **1c** ($\nu_{av} = 2012.5\ cm^{-1}$) and **1f** (2012.0 cm^{-1}).[9] Thus, TEPs do not reflect the widely differing nucleophilicities and Lewis basicities (see below) of mNHOs **1c** and **1g**, which limits the general applicability of TEP as a predictive tool for the nucleophilic properties of mNHOs.

Quantum-Chemical Calculations

Brønsted basicity often correlates poorly with nucleophilicity, in particular when structurally diverse systems with varying functional groups and charges are compared.[30–32] Alternatively, methyl cation affinities (MCAs), defined as the negative Gibbs energies ΔG_{298} of a reaction of a nucleophile with a methyl cation, were supposed to reflect more closely the kinetically observed bond formations. According to an extensive analysis by Baldi, Van Vranken and co-workers, MCAs of neutral and negatively charged (in majority C-centered) nucleophiles correlate well with their nucleophilic reactivities ($N \cdot s_N$) when a COSMO(∞) solvent model was applied in the quantum-chemical calculations.[33]

In an analogous approach, we calculated MCAs of mNHOs **1a–1h** (Figure 6A, C)[34] with the SMD continuum solvation model for THF at the B3LYP/def2-TZVPP//BLYP/def2-TZVPP level of theory. The correlation of nucleophilicity *N* with MCA values was generally good for

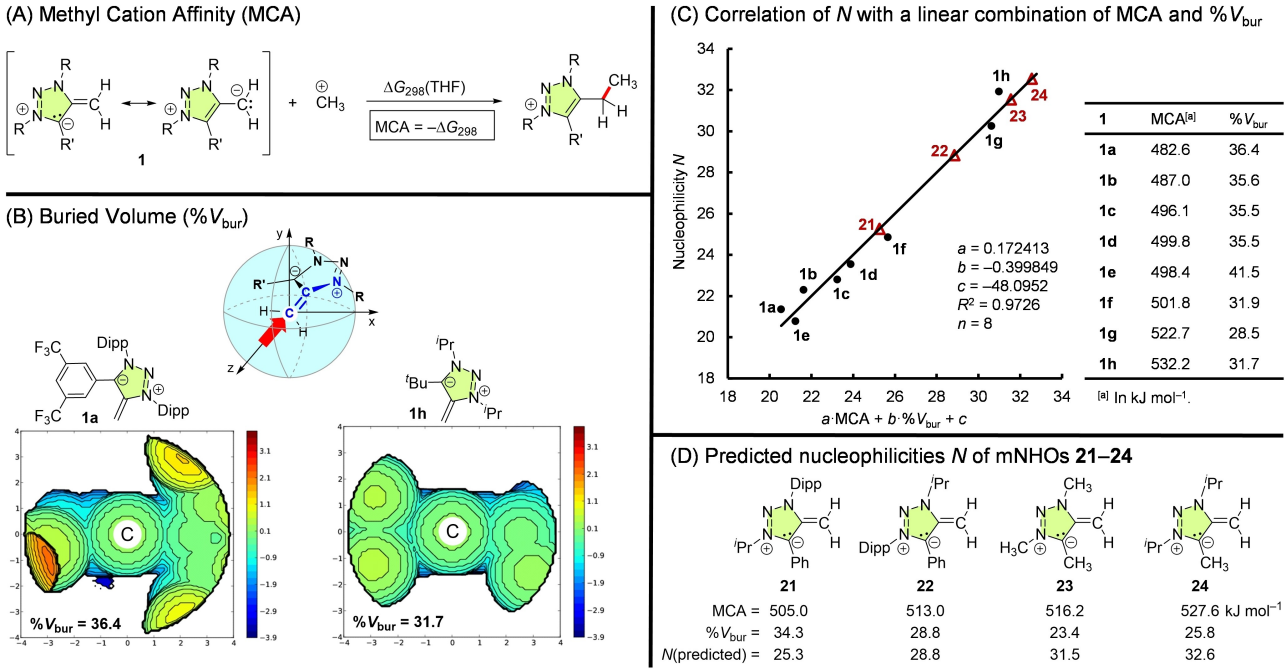

1	MCA[a]	%V_{bur}
1a	482.6	36.4
1b	487.0	35.6
1c	496.1	35.5
1d	499.8	35.5
1e	498.4	41.5
1f	501.8	31.9
1g	522.7	28.5
1h	532.2	31.7

[a] In kJ mol⁻¹.

Figure 6. (A) Defining reaction for Methyl Cation Affinities (MCAs) calculated in this work at the B3LYP(SMD=THF)/def2-TZVPP//BLYP/def2-TZVPP level of theory. (B) Viewing direction for mapping the buried volumes (%V_{bur}) at the exocyclic CH_2 group of mNHOs as exemplified by topographic steric maps for **1a** and **1h**. (C) Linear relationship of nucleophilicities *N* of **1a–1h** with a linear combination of methyl cation affinities (MCA) and steric (%V_{bur}) descriptors. Triangles for structures **21–24** show nucleophilicities *N* predicted on the basis of the depicted linear correlation line. (D) Hypothetical mNHO molecules **21–24** with calculated MCA and %V_{bur} values and predicted nucleophilicities *N*.

© 2023 The Authors. Angewandte Chemie International Edition published by Wiley-VCH GmbH

15213773, 2023, 40, Downloaded from https://onlinelibrary.wiley.com/doi/10.1002/anie.202309790 by Technische Universiteit Dortmund Dezernat Finanzen und Beschaffung, Wiley Online Library on [18/11/2024]. See the Terms and Conditions (https://onlinelibrary.wiley.com/terms-and-conditions) on Wiley Online Library for rules of use; OA articles are governed by the applicable Creative Commons License

the mNHOs **1a**–**1h** ($R^2 = 0.8895$). However, the mNHO **1e**, which carries the sterically demanding Tripp substituent, was an obvious outlier (Supporting Information, p. S146).

Hence, we used the optimized structures from the MCA calculations to determine buried volumes ($\%V_{bur}$)[35] to additionally account for variations of steric bulk at the reactive exocyclic methylene group of the mNHOs (Figure 6B, C).[21] The linear combination of both descriptors, which considers contributions from methyl cation affinities and sterics (that is, $\%V_{bur}$), reliably described the experimental nucleophilicities N for the entire set of the studied mNHOs **1a**–**1h** ($n = 8$, $R^2 = 0.9726$, Figure 6C). On basis of these results, the design of novel mNHOs, such as the depicted mNHO structures **21**–**24**, with predictable nucleophilicities will be possible by resource efficient DFT calculations (Figure 6C, D).[21]

Conclusion

While the persistency of mesoionic *N*-heterocyclic olefins (mNHOs) with bulky 2,6-diisopropylphenyl groups at the nitrogen atoms has been found in earlier work, we now observed that triazole-based mNHOs with a large variety of substituents, including 1,3,5-trialkylated variants, are persistent substances at room temperature. Kinetics of the reactions of mNHOs with arylidene malonates as reference electrophiles showed that their nucleophilicities can be tuned flexibly over a wide range ($N = 20.8$ to 31.9) by variation of the substituents. Alkyl-substituted mNHOs are significantly more nucleophilic than their aryl-substituted counterparts and are presently the strongest nucleophiles on the comprehensive nucleophilicity scale of the Muenchen group, which currently includes >1000 C-, N-, O-, P-, S-, and Se-nucleophiles as well as almost 200 hydride donors.[18] Tolman electronic parameters do not reveal the outstandingly high nucleophilicities of alkyl substituted mNHOs. The nucleophilicity parameters N of the mNHOs correlate well with a linear combination of their methyl cation affinities (that is, DFT-calculated Lewis basicities) and buried volumes (that is, steric hinderance at the reaction center) which facilitates the design of novel mNHO structures with predictable, tailor-made reactivity and affinity towards electrophiles. Since exemplary studies showed that rates and products of the reactions of mNHOs with various electrophilic reaction partners (Michael acceptors, carbon dioxide, electrophilic fluorination reagents) can correctly be predicted by using the reactivity parameters N and s_N, we conclude that these parameters represent a reliable basis for a systematic investigation of the synthetic potential of this new class of compounds.

Acknowledgements

We are grateful to Dr. Julian Holstein (TUD) and Dr. Peter Mayer (LMU) for help with X-ray measurements and analysis. We thank the Deutsche Forschungsgemeinschaft (NMR: DFG project 452669591) under Germany's Excellence Strategy—EXC2033—project number 390677874-RESOLV and the Emmy-Noether program (HA 8832/1-1). Funded/Co-funded by the European Union (ERC, CC-CHARGED, 101077332). The authors gratefully acknowledge the computational and data resources provided by the Leibniz Supercomputing Centre (www.lrz.de). This research was funded in whole, or in part, by the Austrian Science Fund (FWF), project no. J-4592 (Erwin Schrödinger fellowship to A.E.). For the purpose of open access, the author has applied a CC BY public copyright license to any Author Accepted Manuscript version arising from this submission. Open Access funding enabled and organized by Projekt DEAL.

Conflict of Interest

The authors declare no conflict of interest.

Data Availability Statement

The data that support the findings of this study are available in the supplementary material of this article.

Keywords: DFT Calculations · Kinetics · Mesoionic Compounds · Methyl Cation Affinities

[1] Z.-T. Huang, M.-X. Wang, *"1,1-Enediamines" in The chemistry of enamines Part 2* (Ed.: Z. Rappoport), Wiley, Chichester, **1994**, Chap. 22, pp. 1303–1363.
[2] a) U. Gruseck, M. Heuschmann, *Chem. Ber.* **1987**, *120*, 2053–2064; b) G. Ye, S. Chatterjee, M. Li, A. Zhou, Y. Song, B. L. Baker, C. Chen, D. J. Beard, W. P. Henry, C. U. Pittman Jr, *Tetrahedron* **2010**, *66*, 2919–2927.
[3] N. Kuhn, H. Bohnen, J. Kreutzberg, D. Bläser, R. Boese, *J. Chem. Soc. Chem. Commun.* **1993**, 1136–1137.
[4] For reviews on *N*-heterocyclic olefins (NHOs), see: a) R. D. Crocker, T. V. Nguyen, *Chem. Eur. J.* **2016**, *22*, 2208–2213; b) R. S. Ghadwal, *Dalton Trans.* **2016**, *45*, 16081–16095; c) M. M. D. Roy, E. Rivard, *Acc. Chem. Res.* **2017**, *50*, 2017–2025; d) S. Naumann, *Chem. Commun.* **2019**, *55*, 11658–11670.
[5] U. Kaya, U. P. N. Tran, D. Enders, J. Ho, T. V. Nguyen, *Org. Lett.* **2017**, *19*, 1398–1401.
[6] a) C. Hering-Junghans, P. Andreiuk, M. J. Ferguson, R. McDonald, E. Rivard, *Angew. Chem. Int. Ed.* **2017**, *56*, 6272–6275; b) M. K. Sharma, S. Blomeyer, B. Neumann, H.-G. Stammler, M. van Gastel, A. Hinz, R. S. Ghadwal, *Angew. Chem. Int. Ed.* **2019**, *58*, 17599–17603.
[7] P. Walther, A. Krauß, S. Naumann, *Angew. Chem. Int. Ed.* **2019**, *58*, 10737–10741.
[8] a) A. Fürstner, M. Alcarazo, R. Goddard, C. W. Lehmann, *Angew. Chem. Int. Ed.* **2008**, *47*, 3210–3214; b) B. Maji, M. Horn, H. Mayr, *Angew. Chem. Int. Ed.* **2012**, *51*, 6231–6235; c) H. Mayr, S. Lakhdar, B. Maji, A. R. Ofial, *Beilstein J. Org. Chem.* **2012**, *8*, 1458–1478; d) K. Powers, C. Hering-Junghans, R. McDonald, M. J. Ferguson, E. Rivard, *Polyhedron* **2016**, *108*, 8–14; e) Z. Wang, Q.-H. Niu, X.-S. Xue, P. Ji, *J. Org. Chem.* **2020**, *85*, 13204–13210; f) Z. Li, P. Ji, J.-P. Cheng, *J. Org. Chem.* **2021**, *86*, 2974–2985.
[9] M. M. Hansmann, P. W. Antoni, H. Pesch, *Angew. Chem. Int. Ed.* **2020**, *59*, 5782–5787.

© 2023 The Authors. Angewandte Chemie International Edition published by Wiley-VCH GmbH

15213773, 2023, 40, Downloaded from https://onlinelibrary.wiley.com/doi/10.1002/anie.202309790 by Technische Universitaet Dortmund Dezernat Finanzen und Beschaffung, Wiley Online Library on [18/11/2024]. See the Terms and Conditions (https://onlinelibrary.wiley.com/terms-and-conditions) on Wiley Online Library for rules of use; OA articles are governed by the applicable Creative Commons License

[10] For acceptor-substituted mesoionic methylides, see: a) C. A. Ramsden, F. Dumitrascu, *Adv. Heterocycl. Chem.* **2022**, *137*, 71–189; b) R. Maity, B. Sarkar, *JACS Au* **2022**, *2*, 22–57; for Breslow systems, see: c) C. Liu, Z. Zhang, L.-L. Zhao, G. Bertrand, X. Yan, *Angew. Chem. Int. Ed.* **2023**, *62*, e202303478; d) W. Liu, L.-L. Zhao, M. Melaimi, L. Cao, X. Xu, J. Bouffard, G. Bertrand, X. Yan, *Chem* **2019**, *5*, 2484–2494.

[11] For mNHOs with =CH(Ph) groups, see: a) Q. Liang, K. Hayashi, D. Song, *Organometallics* **2020**, *39*, 4115–4122; b) Q. Liang, K. Hayashi, Y. Zeng, J. L. Jimenez-Santiago, D. Song, *Chem. Commun.* **2021**, *57*, 6137–6140; c) Q. Liang, K. Hayashi, L. Li, D. Song, *Chem. Commun.* **2021**, *57*, 10927–10930; d) Z.-W. Qu, H. Zhu, R. Streubel, S. Grimme, *Eur. J. Org. Chem.* **2022**, e202200539; e) Q. Liang, D. Song, *Dalton Trans.* **2022**, *51*, 9191–9198.

[12] a) P. W. Antoni, C. Golz, J. J. Holstein, D. A. Pantazis, M. M. Hansmann, *Nat. Chem.* **2021**, *13*, 587–593; b) P. W. Antoni, J. Reitz, M. M. Hansmann, *J. Am. Chem. Soc.* **2021**, *143*, 12878–12885; c) M. M. Hansmann, *Angew. Chem. Int. Ed.* **2023**, *62*, e202304574.

[13] a) Z. Zhang, S. Huang, L. Huang, X. Xu, H. Zhao, X. Yan, *J. Org. Chem.* **2020**, *85*, 12036–12043; b) S. Maji, A. Das, S. K. Mandal, *Chem. Sci.* **2021**, *12*, 12174–12180.

[14] A. Merschel, Y. V. Vishnevskiy, B. Neumann, H.-G. Stammler, R. S. Ghadwal, *Dalton Trans.* **2022**, *51*, 8217–8222.

[15] Q. Liang, Y. Zeng, P. A. Mendez Ocampo, H. Zhu, Z.-W. Qu, S. Grimme, D. Song, *Chem. Commun.* **2023**, *59*, 4770–4773.

[16] S. Huang, Y. Wang, C. Hu, X. Yan, *Chem. Asian J.* **2021**, *16*, 2687–2693.

[17] a) H. Mayr, M. Patz, *Angew. Chem. Int. Ed.* **1994**, *33*, 938–957; b) H. Mayr, T. Bug, M. F. Gotta, N. Hering, B. Irrgang, B. Janker, B. Kempf, R. Loos, A. R. Ofial, G. Remennikov, H. Schimmel, *J. Am. Chem. Soc.* **2001**, *123*, 9500–9512; c) H. Mayr, B. Kempf, A. R. Ofial, *Acc. Chem. Res.* **2003**, *36*, 66–77; d) H. Mayr, A. R. Ofial, *SAR QSAR Environ. Res.* **2015**, *26*, 619–646.

[18] The database of Mayr reactivity parameters (N, s_N, and E) is freely accessible at www.cup.lmu.de/oc/mayr/reaktionsdaten-bank2/, (accessed 7th July, 2023).

[19] a) W. Wirschun, M. Winkler, K. Lutz, J. C. Jochims, *J. Chem. Soc. Perkin Trans. 1* **1998**, 1755–1761; b) J. Bouffard, B. K. Keitz, R. Tonner, G. Guisado-Barrios, G. Frenking, R. H. Grubbs, G. Bertrand, *Organometallics* **2011**, *30*, 2617–2627; c) D. Sawaguchi, S. Hayakawa, M. Sakuma, K. Niitsuma, D. Kase, S. Michii, M. Ozawa, Y. Sakai, K. Sakamaki, K. Ueyama, R. Haraguchi, *Asian J. Org. Chem.* **2021**, *10*, 901–905.

[20] G. Guisado-Barrios, J. Bouffard, B. Donnadieu, G. Bertrand, *Angew. Chem. Int. Ed.* **2010**, *49*, 4759–4762.

[21] Details are given in the Supporting Information.

[22] Deposition numbers 2271958 (for **1g**), 2271959 (for **6a**), 2271960 (for **7c**), 2271961 (for (*E*)-**9b**), 2271962 (for **19a**), and 2271963 (for **20**) contain the supplementary crystallographic data for this paper. These data are provided free of charge by the joint Cambridge Crystallographic Data Centre and Fachinformationszentrum Karlsruhe Access Structures service.

[23] O. Kaumanns, R. Lucius, H. Mayr, *Chem. Eur. J.* **2008**, *14*, 9675–9682.

[24] C. Hansch, A. Leo, D. Hoekman, *Exploring QSAR: Hydrophobic, electronic, steric constants*, American Chemical Society, Washington, DC, **1995**.

[25] a) S. Helmy, S. Oh, F. A. Leibfarth, C. J. Hawker, J. Read de Alaniz, *J. Org. Chem.* **2014**, *79*, 11316–11329; b) F. Stricker, J. Peterson, J. Read de Alaniz, *Org. Synth.* **2022**, *99*, 79–91.

[26] a) D. S. Timofeeva, A. R. Ofial, H. Mayr, *J. Am. Chem. Soc.* **2018**, *140*, 11474–11486; b) for reviews on N–F fluorinating agents: N. Rozatian, D. R. W. Hodgson, *Chem. Commun.* **2021**, *57*, 683–712; c) T. Umemoto, Y. Yang, G. B. Hammond, *Beilstein J. Org. Chem.* **2021**, *17*, 1752–1813.

[27] a) Y.-B. Wang, Y.-M. Wang, W.-Z. Zhang, X.-B. Lu, *J. Am. Chem. Soc.* **2013**, *135*, 11996–12003; b) for DFT-calculated stabilities of NHO carboxylates, see: L. Dong, J. Wen, W. Li, *Org. Biomol. Chem.* **2015**, *13*, 8533–8544; c) for a review on carbon dioxide adducts of NHCs and NHOs, see: L. J. Murphy, K. N. Robertson, R. A. Kemp, H. M. Tuononen, J. A. C. Clyburne, *Chem. Commun.* **2015**, *51*, 3942–3956; d) for CO_2 adduct formation with conventional and mesoionic NHC imines, see: L. F. B. Wilm, T. Eder, C. Mück-Lichtenfeld, P. Mehlmann, M. Wünsche, F. Buß, F. Dielmann, *Green Chem.* **2019**, *21*, 640–648; e) A. Das, P. Sarkar, S. Maji, S. K. Pati, S. K. Mandal, *Angew. Chem. Int. Ed.* **2022**, *61*, e202213614.

[28] Z. Li, R. J. Mayer, A. R. Ofial, H. Mayr, *J. Am. Chem. Soc.* **2020**, *142*, 8383–8402.

[29] H. V. Huynh, *Chem. Rev.* **2018**, *118*, 9457–9492.

[30] a) J. O. Edwards, *J. Am. Chem. Soc.* **1954**, *76*, 1540–1547; b) F. G. Bordwell, T. A. Cripe, D. L. Hughes, in *Nucleophilicity* (Eds.: J. M. Harris, S. P. McManus), American Chemical Society, Washington, DC, **1987**, pp. 137–153; c) T. A. Nigst, A. Antipova, H. Mayr, *J. Org. Chem.* **2012**, *77*, 8142–8155; d) F. An, B. Maji, E. Min, A. R. Ofial, H. Mayr, *J. Am. Chem. Soc.* **2020**, *142*, 1526–1547.

[31] In ref. [32], Naumann and co-workers suggest to classify NHO basicities by DFT calculated proton affinities. Calculated gas phase proton affinities (PAs) of mNHOs at the BLYP/def2-TZVPP level correlate only within the 4-aryl-substituted *N*-Dipp derivatives **1a**-**1d** with nucleophilicity N but scatter significantly when the whole data set of mNHOs **1a**-**1h** is considered (see Supporting Information).

[32] R. Schuldt, J. Kästner, S. Naumann, *J. Org. Chem.* **2019**, *84*, 2209–2218.

[33] D. Kadish, A. D. Mood, M. Tavakoli, E. S. Gutman, P. Baldi, D. L. Van Vranken, *J. Org. Chem.* **2021**, *86*, 3721–3729.

[34] The resonance structures of the mNHOs suggest nucleophilic reactivity also at the triazole ring. We, therefore, calculated additional MCA values for ring methylations at **1a**, the weakest nucleophile in our study, and at **1h**, the strongest nucleophile. The MCAs at ring positions for both molecules are at minimum by 127 kJ mol^{-1} lower than those for methylation at the exocyclic carbon (Supporting Information). Hence, we considered the contribution of the ring positions to the reactivity of mNHOs as being negligible.

[35] a) L. Falivene, R. Credendino, A. Poater, A. Petta, L. Serra, R. Oliva, V. Scarano, L. Cavallo, *Organometallics* **2016**, *35*, 2286–2293; b) L. Falivene, Z. Cao, A. Petta, L. Serra, A. Poater, R. Oliva, V. Scarano, L. Cavallo, *Nat. Chem.* **2019**, *11*, 872–879; c) buried volumes (%V_{bur}) were determined by using the *SambVca 2.1* web application: https://www.molnac.unisa.it/OMtools/sambvca2.1/ (accessed 31/07/2023).

Manuscript received: July 10, 2023
Accepted manuscript online: August 4, 2023
Version of record online: August 29, 2023

© 2023 The Authors. Angewandte Chemie International Edition published by Wiley-VCH GmbH

15213773, 2023, 40, Downloaded from https://onlinelibrary.wiley.com/doi/10.1002/anie.202309790 by Technische Universitaet Dortmund Dezernat Finanzen und Beschaffung, Wiley Online Library on [18/11/2024]. See the Terms and Conditions (https://onlinelibrary.wiley.com/terms-and-conditions) on Wiley Online Library for rules of use; OA articles are governed by the applicable Creative Commons License